Enhancement of Intersubband Absorption in GaInN/AlInN Quantum Wells

G. Cywiński[a], C. Skierbiszewski[a], M. Siekacz[a],
A. Feduniewicz-Żmuda[b], M. Kryśko[a], M. Gladysiewicz[c],
R. Kudrawiec[c], L. Nevou[d], N. Kheirodin[d], F.H. Julien[d]
and J. Misiewicz[c]

[a]Institute of High Pressure Physics, Polish Academy of Sciences
Sokołowska 29/37, 01-142 Warsaw, Poland
[b]TopGaN Ltd, 01-142 Warsaw, Poland
[c]Institute of Physics, Wrocław University of Technology, 50-370 Wrocław, Poland
[d]Action OptoGaN, Institut d'Electronique Fondamentale, Université Paris-Sud
UMR 8622, CNRS, 91405 Orsay Cedex, France

GaInN/AlInN multiple quantum wells were grown by RF plasma-
-assisted molecular beam epitaxy on (0001) GaN/sapphire substrates. The
strain-engineering concept was applied to eliminate cracking effect and to
improve optical parameters of intersubband structures grown on GaN sub-
strates. The high quality intersubband structures were fabricated and inves-
tigated as an active region for applications in high-speed devices at telecom-
munication wavelengths. We observed the significant enhancement of in-
tersubband absorption with an increase in the barrier thickness. We at-
tribute this effect to the better localization of the second electron level in
the quantum well. The strong absorption is very important on the way to
intersubband devices designed for high-speed operation. The experimental
results were compared with theoretical calculations which were performed
within the electron effective mass approximation. A good agreement be-
tween experimental data and theoretical calculations was observed for the
investigated samples.

PACS numbers: 78.30.Fs, 78.67.De, 68.65.Fg, 73.21.Fg, 81.15.Hi

1. Introduction

The Al(In)N/Ga(In)N material system, with its large conduction band dis-
continuity of ≈ 1.9 eV, attracts increasing attention for intersubband (IS) devices

operating at the technologically interesting wavelength range around 1.55 [1–11]. The true application potential of nitrides, however, is most likely related to its ultra-short IS scattering times of the order of 140 fs [8]. Unipolar devices relying on IS transitions open new perspective for ultrafast fiber optoelectronic, where using them a significant increase in the bit rate in a single channel of the fiber could be achieved. However, in spite of many scientific efforts in research laboratories the development of high speed IS devices is still an open issue [9, 12]. The main problem is the big lattice mismatch between AlN and GaN, which can lead to the appearance of cracks or defects. One can overcome the cracking and defects problems [13, 14] using the strain engineering of AlInN/GaInN multiple quantum wells (MQWs) and the GaN substrate [10, 15]. The successful growth of high quality IS structures on GaN substrates opens new perspectives for IS devices. In this way the IS structures are not limited of poor quality of AlN substrates or problems with doping of high aluminum content AlGaN layers.

We present our recent results for IS absorption of AlInN/GaInN structures, which fulfill optical requirements for the device application. Due to partially strain compensation we were able to increase the barrier width which apparently amplify the strength of IS absorption at telecommunication wavelengths. The obtained absorption is especially attractive for the ultrafast IS devices, where small sizes of the mesa are required.

To explain the enhancement of IS absorption we compare the experimental data with theoretical calculations. We will discuss a possible explanation of this physical phenomenon. The proper understanding of it could facilitate the appropriate design of devices.

2. Experiment

In this paper we present our results obtained for AlInN/GaInN IS structures. The structures have been grown with plasma assisted molecular beam epitaxy (PAMBE) on Ga polar GaN/Al_2O_3 templates. More details on the growth procedure and structural investigations can be found in Refs. [10, 15]. The recent improvement of our technology and design IS structures resulted in a large increase in IS absorption per one quantum well. For this communication we have compared the results obtained for two similar IS structures. Our structures are presented in Fig. 1. The both samples have the same quantum well (QW) thickness and QWs were uniformly doped with Si at a level of 1×10^{20} cm^{-3}. The main difference between sample A and sample B (reference sample) is the quantum well barrier thickness. The barrier thicknesses of samples A and B are 5.5 and 2.2 nm, respectively. These IS structures have been characterized by X-ray diffractometry (XRD) (Fig. 2). We observed several satellite peaks from the AlInN/GaInN superlattice. This large amount of satellite peaks confirms very good periodicity of the structure. We used simulations for the ideal layered structures to determine the period of MQWs and to approximate the layer compositions. The good
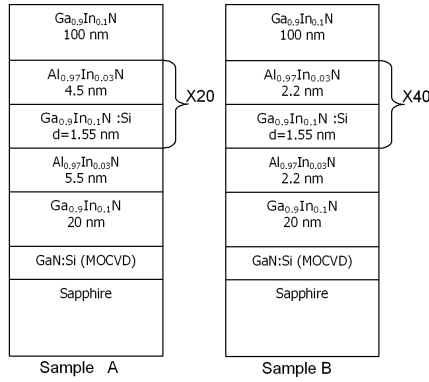
| Ga$_{0.9}$In$_{0.1}$N 100 nm |
| Al$_{0.97}$In$_{0.03}$N 4.5 nm |
| Ga$_{0.9}$In$_{0.1}$N :Si d=1.55 nm |
| Al$_{0.97}$In$_{0.03}$N 5.5 nm |
| Ga$_{0.9}$In$_{0.1}$N 20 nm |
| GaN:Si (MOCVD) |
| Sapphire |

Fig. 1. Layer structures of AlInN/GaInN MQW samples.
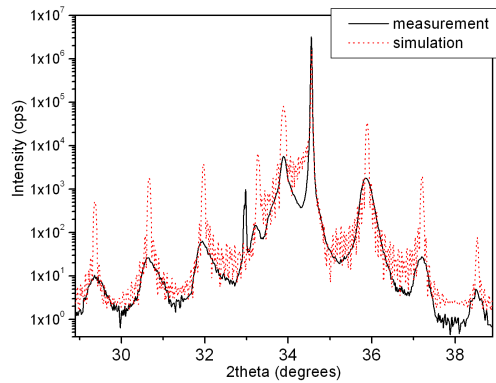
Fig. 2. Result of XRD measurements made on Al$_{0.93}$In$_{0.07}$N/Ga$_{0.9}$In$_{0.1}$N IS structure (continuous line) and numerical simulation (dotted line), which confirms the assumed structure.

agreement between experimental data and simulation shows a good quality of the structure. To determine strain and relaxation of the layers, we used the XRD mapping technique (which detects the change of lattice parameters c and a). The result of XRD mapping is shown in Fig. 3. Here one can see layer and superlattice peaks which are partially relaxed to the GaN substrate. We have used the data of XRD reciprocal space mapping and simulations as an input to the theoretical calculations.

The absorption experiments were performed in the Fourier transform infrared (FTIR) setup at room temperature. The samples were prepared for the geometry measurement of the multipass waveguide. Prepared samples are placed at Brewster's angle with respect to the incident beam of the FTIR. The incident light is either s-polarized (TE) or p-polarized (TM). The more details can be found in [10, 15]. The results of IR transmission are shown in Fig. 4. The upper inset shows the scheme of the IS measurement and light polarizations. The left part of
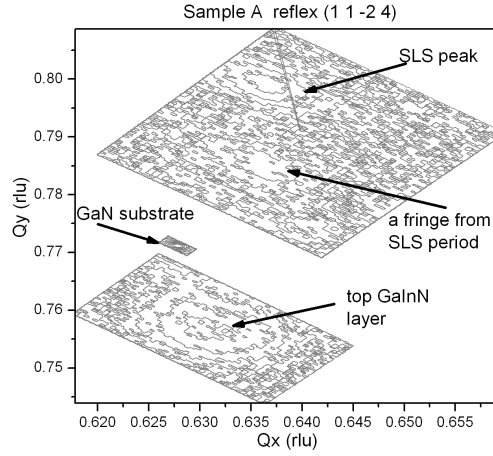
Fig. 3.   The reciprocal space map of the sample A. The XRD measurement shows the strain state of the layered structure of the sample.
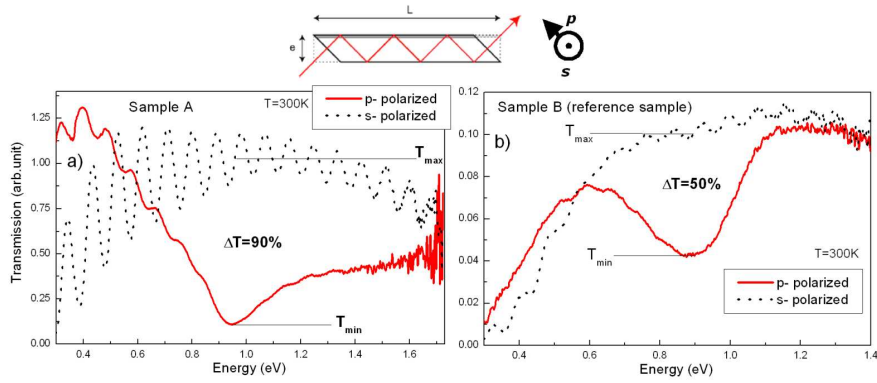

Fig. 4.   Room temperature transmission measurements for *p*-polarized (solid line) and *s*-polarized (dotted line) light. The measurements were done in multipass waveguide geometry schematically presented in the upper part of the figure. Sample A shows enhanced IS absorption, results of IS transmission of sample B is presented for the comparison. T was calculated using the formula $T = 100\% \times (T_{max} - T_{min})/T_{max}$.

this figure shows the transmission result of the sample A. One can see the strong IS absorption (90%). The calculated IS absorption per one pass of the QW is 0.17%. The right part of the figure presents the IS transmission for the reference sample (sample B). Barriers, in this reference sample, are two times thinner and the amount of QWs is doubled. For this sample IS absorption is much lower i.e. 50% which corresponds to the value 0.048% calculated per one QW pass. In comparison with the sample A the reference sample shows the 3.5 times weaker IS absorption. The IS absorption of the sample A, because of the exceptional strong absorption, has been measured at Brewster's angle of incidence. Figure 5 shows
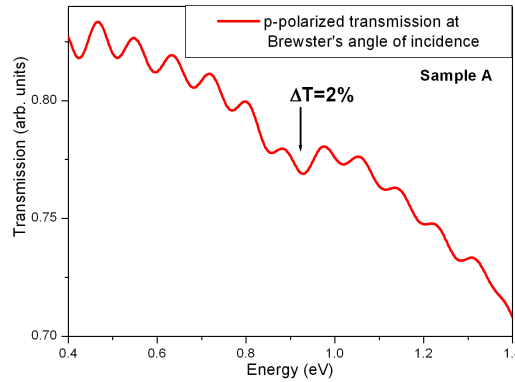
Fig. 5. Room temperature transmission measurements at Brewster's angle of incidence for sample A. The presented data for p-polarized light shows 2% of IS absorption.

the transmission, where the arrow indicates the position of the IS absorption. Strong Fabry–Perot oscillations, which are visible in Fig. 5, are ascribed to multireflections between the surface and the interface GaN/sapphire. Nevertheless the IS absorption is clearly evident in this figure.

3. Theoretical calculations and comparison with IS experiments

The experimental results have been compared with theoretical calculations which were performed within the standard electron effective mass approximation. In order to find the electron confinement potential, we have considered spontaneous and piezoelectric polarizations in this system with material parameters taken after Ref. [16]. It has been assumed that the total potential drop in one period of the structure equals zero and the electric field in the QW and barrier was calculated according to this assumption [17]. We have considered two situations: the first one with the QW width of 1.55 nm and the barrier width of 6 nm and the second one with the same QW width and twice narrower barrier width (i.e. 3 nm width barrier). The two situations correspond to two samples which are considered in this paper. In a real system the shape of electron potential can be a little bit different due to uncertainty in material parameters, etc., but trends in the calculations can be extrapolated to a real system, i.e. the two MQWs which are considered in this paper. A detailed theoretical analysis for this system will be presented elsewhere.

Figure 6 shows the confinement potential for GaInN/AlInN QWs together with the modulus of electron wave functions for the first and the fourth electron levels (let us note that from the "calculation" point of view, it is a system of three QWs embedded in a deep QW). It is clearly visible in this figure that the coupling between QWs is negligible for the system with 6 nm wide barriers. In this case, the electron wave functions are localized in one QW region and each QW can be considered independently. The coupling between QWs starts to be important for QWs with narrower barriers. In this case, the energy coupling for
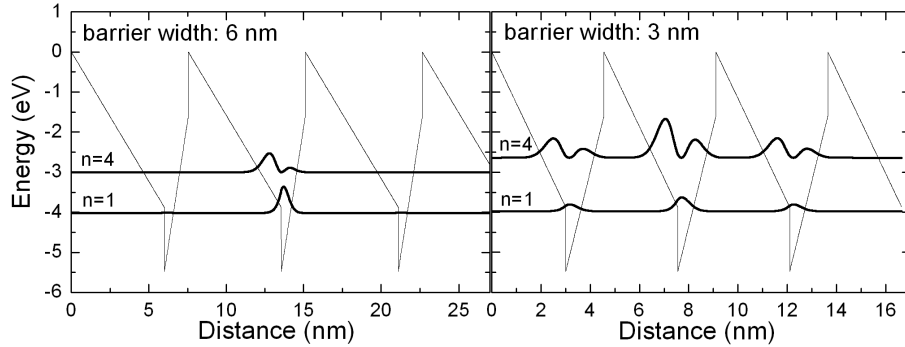
Fig. 6. Electron confinement potential together with energy levels and modulus of electron wave function for the first and the fourth electron and levels.

the ground state transition (the energy difference between the first and the third electron levels) is small (< 1 meV) but the electron wave functions are distributed through all three QWs. In the case of the excited states ($n > 3$), the potential of AlInN barrier drops below the energy of this state (see Fig. 6) and therefore the excited states should be treated as semi-confined and/or above-barrier states. It is expected that the oscillator strength is stronger for the first situation where both states (the ground and excited ones) are strongly localized in one QW. In the case of the second situation the intersubband absorption can be weaker since it is an absorption between localized states and semilocalized states. We believe that the situation realized in our samples is very similar to this which was analyzed theoretically.

4. Conclusions

The results of IS absorption experiments for AlInN/GaInN are attractive for ultrafast devices. Due to the strain engineering concept we overcame the cracking problem for thick barriers on GaN substrates. We found a significant increase in IS absorption with the increase in the barrier width. We attribute this effect to the better localization of electron levels in the QW region, i.e., each QW can be treated independently for a system with wider barriers. Further experimental and theoretical works are required to the better precision of structure parameters and improve the device design.

Acknowledgments

References

[1] C. Gmachl, H.M. Ng, S. Chu, A.Y. Cho, *Appl. Phys. Lett.* **77**, 3722 (2000).

[2] N. Iizuka, K. Kaneko, N. Suzuki, T. Asano, S. Noda, O. Wada, *Appl. Phys. Lett.* **77**, 648 (2000).

[3] H.M. Ng, C. Gmachl, S.N.G. Chu, A.Y. Cho, *J. Cryst. Growth* **220**, 432 (2000).

[4] N. Iizuka, K. Kaneko, N. Suzuki, *Compound Semiconductors 2004 Proceedings of the Thirty First International Symposium on Compound Semiconductors Institute of Physics Conferences Series* **No 184**, 115 (2005).

[5] N. Iizuka, K. Kaneko, N. Suzuki, *Opt. Express* **13**, 10 (2005).

[6] E. Baumann, F.R. Giorgetta, D. Hofstetter, H. Wu, W.J. Schaff, L.F. Eastman, L. Kirste, *Phys. Status Solidi C* **3**, 1014 (2005).

[7] S. Matsui, Y. Ishii, T. Morita, P. Holmstrom, H. Sekiguchi, A. Kikuchi, K. Kishino, *Phys. Status Solidi C* **7**, 2748 (2005).

[8] J. Hamazaki, S. Matsui, H. Kunugita, K. Ema, H. Kanazawa, T. Tachibana, A. Kikuchi, K. Kishino, *Appl. Phys. Lett.* **84**, 1102 (2004).

[9] F.R. Giorgetta, E. Bauman, F. Guillot, E. Monroy, D. Hofstetter, *Electron. Lett.* **43**, 185 (2007).

[10] G. Cywinski, C. Skierbiszewski, A. Feduniewicz-Zmuda, M. Siekacz, L. Nevou, L. Doyennette, M. Tchernycheva, F.H. Julien, P. Prystawko, M. Krysko, S. Grzanka, I. Grzegory, A. Presz, J.Z. Domagała, J. Smalc, M. Albrecht, T. Remmele, S. Porowski, *J. Vac. Sci. Technol.* **24**, 1505 (2006).

[11] M. Tchernycheva, L. Nevou, L. Doyennette, F.H. Julien, E. Warde, F. Guillot, E. Monroy, E. Bellet-Amalric, T. Remmele, M. Albrecht, *Phys. Rev. B* **73**, 125347 (2006).

[12] C. Kumtornkittikul, T. Shimizu, N. Iizuka, N. Suzuki, M. Sugiyama, Y. Nakano, *J. J. Appl. Phys. Part-2-Lett.* **46**, L352-5 (2007).

[13] E.A. DeCuir Jr., Y.C. Chua, B.S. Passmore, J. Liang, M.O. Manasreh, J. Xie, H. Morkoc, A. Asghar, I.T. Ferguson, A. Payne, *Progress in Compound Semiconductor Materials IV Electronic and Optoelectronic Applications Symposium Materials Research Society Symposium Proceedings* **829**, 175 (2005).

[14] J. Dorsaz, J. Carlin, S. Gradecak, M. Ilegems, *J. Appl. Phys.* **97**, 84505 (2005).

[15] G. Cywinski, C. Skierbiszewski, A. Feduniewicz-Zmuda, M. Siekacz, L. Nevou, L. Doyennette, F.H. Julien, P. Prystawko, M. Krysko, S. Grzanka, I. Grzegory, S Porowski, *Acta Phys. Pol. A* **110**, 175 (2006).

[16] I. Vurgaftman, J.R. Meyer, *J. Appl. Phys.* **94**, 3675 (2003).

[17] V. Fiorentini, F. Bernardini, F.D. Sala, A.D. Carlo, P. Lugli, *Phys. Rev. B* **60**, 8849 (1999).